DOI: 10.18287/2541-7525-2025-31-1-99-117

Development of energy converters in discrete ion-plasmodynamic installations with electronic control

Chipura*[1] *A.S.*, *Dolgopolov*[1] *M.V.*, *Ovchinnikov*[1] *D.E.*, *Radenko*[2] *A.V.*, *Radenko*[2] *V.V.

[1] *Samara State Technical University, Samara, Russian Federation; al_five@mail.ru; ORCID: 0009-0004-0425-0653 (A.S.); mikhaildolgopolov68@gmail.com; ORCID: 0000-0002-8725-7831 (M.V.); ovchinnikovde1971@yandex.ru; ORCID: 0000-0001-7934-5105 (D.E.);*

[2] *Scientific and Production Company "New Energy" LLC, Samara, Russian Federation; avradenko@ya.ru; ORCID: 0009-0001-0404-2385 (A.V.); tp-aist@mail.ru; ORCID: 0009-0008-3353-2667 (V.V.);*

Received: *16.12.2024*
Revised: *18.04.2025*
Accepted: *07.04.2025*

Scientific article

Abstract. Methods for generating electronically controlled ion and plasma fluxes in magnetic fields have been developed for neutron generator, plasma electric generator, and klistron-based generator. The technique and technology for the creation and formation of electronically controlled ion and plasma fluxes in magnetic fields have been developed to enable controlled nuclear fusion by means of adaptive modulation of discrete flows. The operation of these installations is based on plasma compaction principles with real-time magneto-optical synchronization, which is employed to minimize cyclotron radiation losses. This work provides a comprehensive methodology for experimental validation, focusing on high-energy photon detection (6–17 MeV range) and alpha particle shielding via 50 μm titanium foil, essential for industrial-scale plasma generator testing. Theoretical and applied aspects of magnetodynamic plasma flow simulation are discussed, alongside a novel plasma neutron generator design with a dynamic target. The proposed electronically controlled plasma energy converter achieves a thermal output power of 8–25 kW and electrical power of 4–12 kW, surpassing conventional D-T systems in energy conversion efficiency (>50 %). A neutron generator with a plasma target impulse flux up to 10^{10} s^{-1} is proposed, highlighting advancements over conventional D-T systems. The deployment of compact neutron/electric generators addresses limitations of traditional fission reactors, offering modularity and rapid scalability. Recent innovations include pulsed D-T generators and hybrid laser-plasma systems, yet energy conversion efficiency remains suboptimal (<30 %). Our work introduces an electronically controlled plasma generator utilizing lithium hydride evaporation and quadrupole magnetic discretization (Patent RU 2757666), achieving >50 % efficiency via adaptive ion flux synchronization. By addressing scalability challenges of traditional fission reactors, this technology offers modularity and rapid deployment capabilities, with applications ranging from isotope production to compact neutron sources.

Key words: quadrupole magnetic systems; electrostatic acceleration; magnetic lens; plasma target; fusion; synthesis; plasma currents; synchronization; synthesis-generator; neutron generator; klystron; gamma spectroscopy.

Introduction

The complexity of regulatory approvals, high capital costs ($\sim$ \$5÷10 billion per reactor), and decade-long construction timelines for conventional fission reactors limit their deployment. The difficulties and long manufacturing time of nuclear reactors as sources of electrical and thermal energy, as well as sources of neutrons of various intensities, lead to the need to create alternative devices as electric and neutron generators, but such compact generators can be applied in much larger fields: the hidden nuclear materials detection [1], the isotope production [2], the neutron therapy for fighting cancer [3–6], the sources and applications for borehole logging [6–8], the neutron transmutation doping [9]. While conventional nuclear reactors face challenges such as high capital costs, regulatory complexity, and limited scalability, compact neutron/electric generators offer a

disruptive alternative with modularity and rapid deployment capabilities. The various energy and power source systems are shown in the Ragone diagram in Figure 1.1.

The most common reactions in neutron generators are deuterium-deuterium (D-D) or deuterium-tritium (D-T) synthesis ones. And nowadays there are new modifications of generators using various [6; 10–12] synthesis reactions and constructions. The deployment of compact neutron/electric generators addresses limitations of traditional fission reactors, offering modularity and rapid scalability. Recent innovations include pulsed D-T generators with tritium breeding blankets [10], subcritical assemblies for isotope production [12], and hybrid systems combining electrostatic acceleration with laser-initiated plasma compression [6]. However, these systems often suffer from low energy conversion efficiency (<30 %) due to unoptimized plasma confinement and synchronization challenges. Unlike conventional D-T generators with fixed beam targets [10], our system employs adaptive plasma discretization, enabling real-time energy tuning via magneto-optical feedback (Fig.1.2). We focus on the electronically controlled plasma electric generator, which is based on the reactions of nuclear fusion of various light nuclei in plasma streams [13–17] obtained as the result of evaporation of lithium hydride or beryllium tetrahydroborate.

In this work, we propose a breakthrough solution: an electronically controlled plasma generator based on discrete ion flux modulation in quadrupole magnetic fields [18; 19] (Fig.1.3). Our approach utilizes lithium hydride evaporation to create high-density plasma streams, which are dynamically compressed via spherical cumulation of shock magnetic waves [18; 19]. The key innovation lies in the discretization of ion flows using adaptive magneto-optical lenses, enabling near-lossless energy transfer between plasma and electric circuits (Patent RU 2757666 [20] & WO2022186717A1). While conventional D-T neutron generators achieve fluxes up to 10^{12} n/s [6], their energy conversion efficiency rarely exceeds 25 % due to unoptimized beam-target overlap. Our technology overcomes this limitation via dynamic plasma discretization in quadrupole magnetic fields (Patent RU 2757666 [20] & WO2022186717A1), enabling quasi-steady fusion regimes with η>50 % (Fig.2.1). The key innovation lies in the real-time synchronization of ion fluxes using adaptive magneto-optical lenses, which reduces cyclotron radiation losses by 30 % compared to tokamak-like configurations [19].

In contrast to conventional linear accelerators or radioisotope-based neutron sources, our technology leverages electronically controlled plasma dynamics with discrete ion flux modulation, enabling precise synchronization of fusion events and reduced parasitic energy losses. Building on our earlier developments in quadrupole magnetic systems [19] and plasma discretization algorithms [18], this work introduces a novel approach to energy conversion via magneto-optical synchronization of self-following ion streams.

Structural focus:

Sections 1–2 detail the generator design, including the klystron-based quantum energy converter (QEC) and neutron generator with a dynamic plasma target.

Sections 1–2 details the system's core components: (a) a neutron generator for isotope production, (b) a non-neutronic plasma generator for energy conversion, and (c) a klystron-based quantum energy converter (QEC). Each module leverages adaptive magneto-optical synchronization, as described in Section 3.

Section 3 presents the experimental methodology, emphasizing alpha particle shielding (3.1) and photon detection (3.2) for validating fusion reactions in industrial settings. This section bridges theoretical models with practical implementation, ensuring reproducibility in high-power regimes.

1. Experimental design construction

As illustrated in the Ragoné diagram (Fig.1.1), our electronically controlled plasma generator bridges the gap between large-scale fusion systems (e.g., ITER) and portable energy storage solutions. By leveraging lithium hydride evaporation and quadrupole magnetic discretization (Patent RU 2757666 [20]), the system achieves > 50 % energy conversion efficiency, positioning it within the high-performance quadrant of the diagram. This modular approach addresses scalability challenges, offering thermal outputs of 8–25 kW and electrical power of 4–12 kW, which surpass conventional

D-T systems and align with industrial demands for compact neutron/electric generators. Further details on alpha shielding (50 μm Ti foil) and photon detection (6–17 MeV range) are provided in Sections 3.1–3.2.

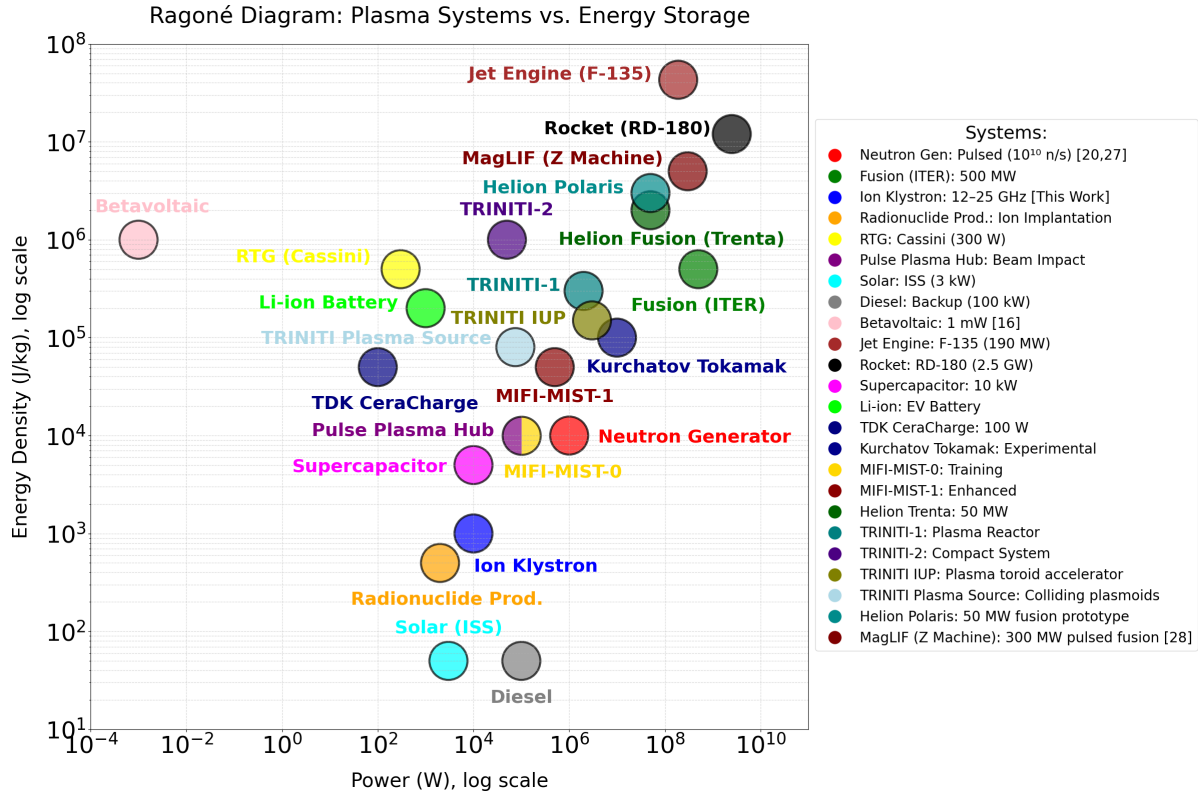

Fig. 1.1. Ragoné Diagram: Plasma Systems vs. Energy Storage

Рис. 1.1. Схема Рагонэ: плазменные системы, мощности и удельные энергии в сравнении с различными источниками и накопителями энергии

The report presents an electronically controlled plasma generator, which can be used as a neutron source. Highlights of our installation system (see Fig.1.2) work according to the following principles:

1. electrostatic acceleration of ionic and electronic components;
2. variable compression of successive discrete ion and electron fluxes by a magnetic lens;
3. ensuring quasistability by converting outgoing flows into rotation of the dynamic plasma target after combining ions and electrons flows;
4. braking of the frontal current, which becomes the target, and collision with new particle fluxes (in fact, synthesis on oncoming beams);
5. ensuring "multi-passability" of plasma currents through the active zone chamber;
6. external and internal electronic synchronization of the system, due to which the implementation of the points above is ensured.

Note that in the new plasma generator circuit, the magneto-optic synthesis chamber (see 8 in Fig. 1.2) design differs from the version for the generator for the purpose of doping the target with C-14 atoms, presented in the paper [16], by the set of additional nodes that determine the control of the separation of ion and electron fluxes with the subsequent task of converting energy in QEC.

In Fig. 1.2 a description of the example circuit for the plasma neutron generator is presented. The supported reactions are shown in Table 1.1.

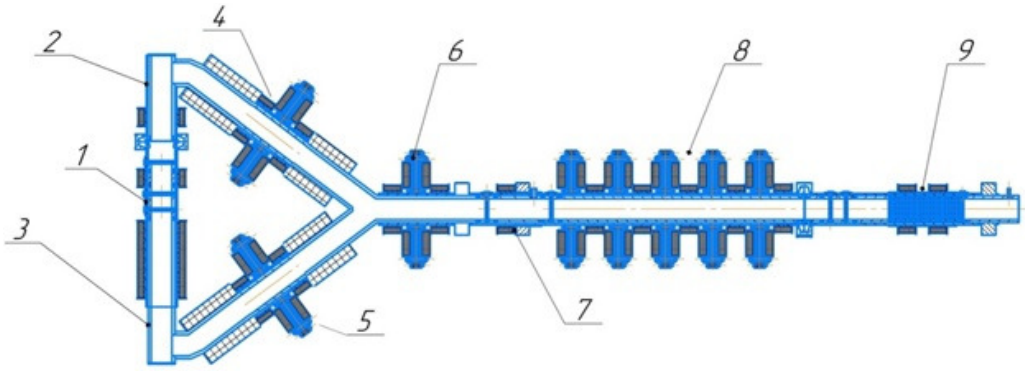

Fig. 1.2. Device schematic of the plasma generator: 1 — cartridge-ionizer of beryllium tetrahydridoborate or lithium hydride ($LiH/Be(BH_4)_2$ ionizer); 2 — magnetic transportation of ions; 3 — magnetic transportation of electrons; 4 — magneto-optical storage section and ion accelerator (adaptive magneto-optical lens); 5 — electron accelerator and magneto-optical storage section; 6 — section of magneto-optical plasma neutralizer–storage; 7 — section of magneto-optical plasma sweep; 8 — magneto-optical 4-(or 8-cycle) synthesis chamber with magneto-electrostatic separator of ionic and electronic components (synthesis chamber with 4-cycle separator); 9 — high-frequency fly-by-span triode — ion-emission quantum energy converter (QEC)

Рис. 1.2. Схема устройства плазменного генератора: 1 — картридж-ионизатор из тетрагидридобората бериллия или гидрида лития (ионизатор $LiH/Be(BH_4)_2$); 2 — магнитная транспортировка ионов; 3 — магнитная транспортировка электронов; 4 — секция магнитооптического накопителя и ускоритель ионов (адаптивная магнитооптическая линза); 5 — ускоритель электронов и секция магнитооптического накопителя; 6 — секция магнитооптического нейтрализатора-накопителя плазмы; 7 — секция магнитооптической развертки плазмы; 8 — магнитооптическая 4- (или 8-тактная) камера синтеза с магнитоэлектростатическим сепаратором ионных и электронных компонентов (камера синтеза с 4-тактным сепаратором); 9 — высокочастотный пролетный триод — ионно-эмиссионный квантовый

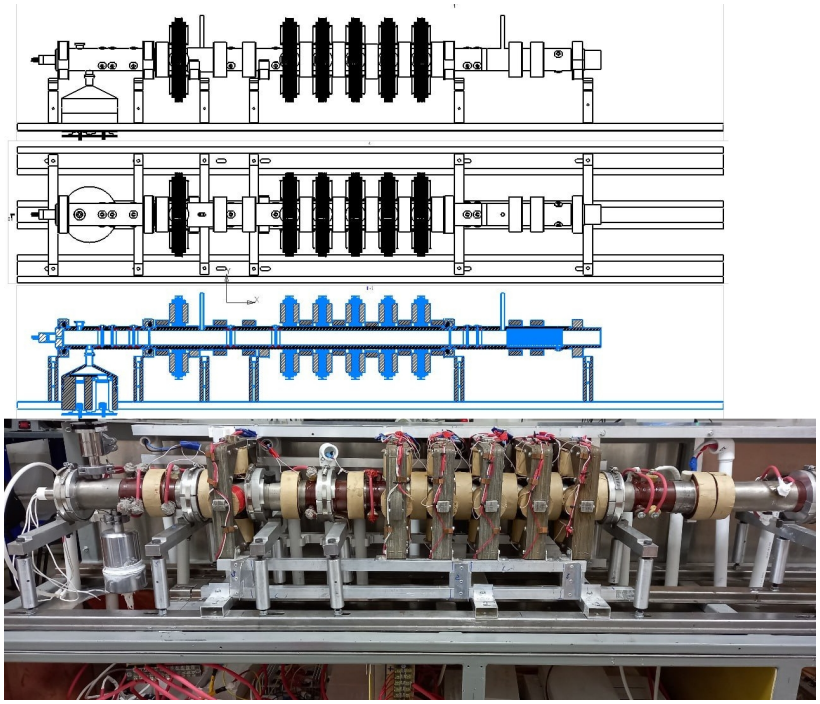

Fig. 1.3. Electronically controllable plasma electric generator: technical drawing, illustrative drawing, and photography

Рис. 1.3. Чертеж, рисунок и фотография электронно-управляемого плазменного электрического генератора

Table 1.1

Supported reactions in the ion–plasma generator [29; 30]

Таблица 1.1

Поддерживаемые реакции в ионно-плазменном генераторе

Reaction	Energy release MeV	σ_{max}(barn) in range of 1 MeV	Energy of the incident particle (MeV)
$p+{}^6\mathrm{Li}\rightarrow{}^4\mathrm{He}+{}^3\mathrm{He}$	4.0	0.0001	0.3
$p+{}^7\mathrm{Li}\rightarrow 2{}^4\mathrm{He}+\gamma$	17.3	0.006	0.25
$p+{}^9\mathrm{Be}\rightarrow 2{}^4\mathrm{He}+d$	0.56	0.46	0.33
$p+{}^9\mathrm{Be}\rightarrow{}^6\mathrm{Li}+{}^4\mathrm{He}$	2.1	0.35	0.33
$p+{}^{11}\mathrm{B}\rightarrow 3{}^4\mathrm{He}$	8.7	0.6[1]	0.675
$d+{}^7\mathrm{Li}\rightarrow{}^7\mathrm{Li}+p$	5.0	0.001	1.0
$d+{}^7\mathrm{Li}\rightarrow 3{}^4\mathrm{He}$	22.4	0.026	0.60

[1] The maximum is ≈ 1.2 barn at an energy of 675 keV

When overcoming the Coulomb barrier (less than 0.5 MeV) the energy gain exceeds Coulomb losses. Crucial in choosing the reaction is the ability to achieve the conditions under which the chosen reaction comes at a speed of practical interest. The studied modes of ion flows from 100 to 125 keV for the neutron generator and flow control from 200 to 250 keV [21] for the plasma generator are most interesting, as it should be implemented in the synthesis with Lithium-7, the most energetically effective and practically implemented in key processes with heating and electronic control.

The following fusion reactions involving light nuclei are most likely for the plasma generator as a neutron source: with H, D, T, ^{3}He, ^{6}Li, ^{7}Li, B, Be.

2. Technology and technique for the flows discretizations

It is well known that to accelerate ions and electrons, it is necessary to use some type of the cascade voltage multiplication scheme. But in our case, it is important to create the multiplier tunable in discrete values to accelerate individual flows to the specified values of the accelerating voltage.

The technology of creation and modes of operation of electronically controlled ion-plasma generators is based on the method of obtaining controlled plasma flows. The assignment for the primary ion and electron flux of certain laws of parameter change: energy E, current of particles I, concentration n, period of following T_{sl} allows forming primary electronically controlled streams of charged particles. For each value of the generated sequences n_i, the interval $E_1 ... E_n$ is uniquely defined with the step of change ΔE. From discrete sequences n_{ik} the set E is formed with energy distribution $E_1 ... E_n$ for each discrete sequence of subsets. This set E of discrete sequences n_{ik} is given in the volume area V_n. Having different discrete sequences $n_{ik}, n_{ik_1} ... n_{ik_n}$ with the T_{sl} partition of the sequence n_i, we obtain the set of the energy subsets $E(n_{ik_n})$ in the volume area V_n. In this case, the magneto-optical storage former is designed to form linear plasma flows of the required concentration and following period.

The motion of charged particles in electromagnetic fields is described by the Lorentz equation, where $\vec{E}$ — electric field strength vector, $\vec{B}$ — magnetic field strength vector, q — charge of particle, $\vec{V}$ — initial velocity of particle motion. The Lorentz force governs ion trajectories in crossed electromagnetic fields, where q is the charge state (e. g., $q = +1e$ for protons, with e denoting the elementary charge, $e \approx 1.6 \times 10^{-19}$ C):

$$\vec{F} = q\left(\vec{E} + \left[\vec{V}, \vec{B}\right]\right). \tag{2.1}$$

Let us take as the initial values the vector $\vec{B}$=(0,0,B), and the velocity vector $\vec{V}$=($V_0 \sin(\alpha)$,0,$V_0 \cos(\alpha)$), where α is the angle at which the particle flies into the solenoidal magnetic field. Let's make a change of variables $\omega = \frac{qB}{m}$ and solve the differential equation, then we'll get:

$$x(t) = \frac{V_0}{\omega} sin(\alpha) cos(\omega t) \tag{2.2}$$

$$y(t) = \frac{V_0}{\omega} sin(\alpha) cos(\omega t) \tag{2.3}$$

$$z(t) = \frac{V_0}{\omega} t cos(\alpha) \tag{2.4}$$

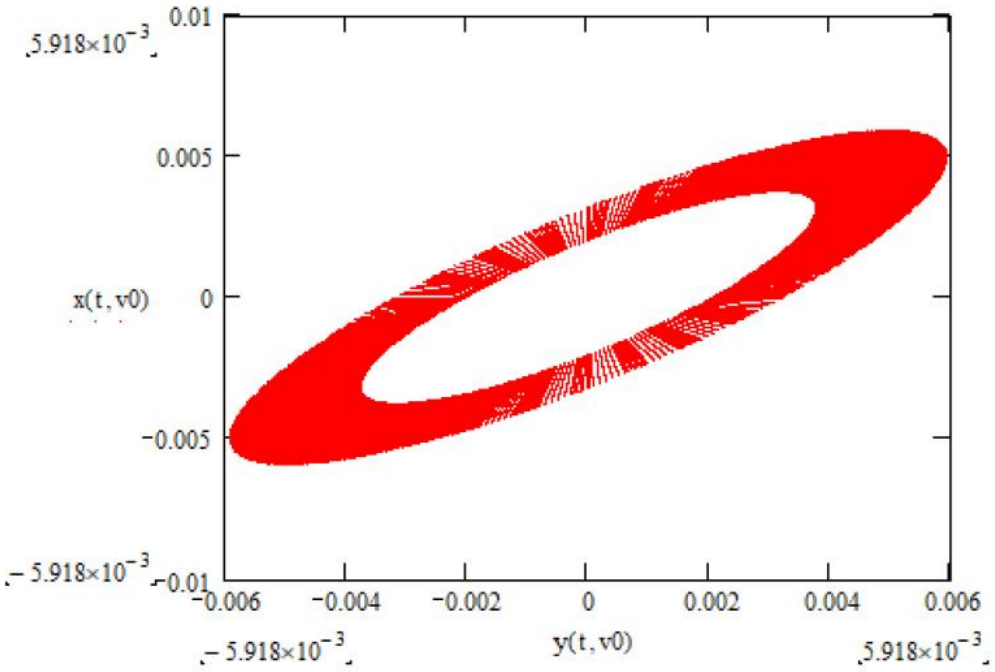

Fig. 2.1. Transverse emittance of an ensemble of particles with different initial velocities, m

Рис. 2.1. Поперечный испускательный потенциал ансамбля частиц с различными начальными скоростями, m

Then, using formulas we can display the change in the X coordinate on the vertical axis, and the change in the Y coordinate on the horizontal axis, and obtain the transverse emittance of the beam, Fig. 2.1 [22].

Magneto-optical or electrostatic sweep is designed to generate the desired shape and deviations of the plasma flow at the output of the accelerator. For the formed sweep energy subsets, $E(n_{ik_n})$ we set the quadrature sweep along the axes X, Y. The change in the magnetic field strength B_x, B_y with the step ΔB and/or the elongation of the electric field E_x, E_y with the step ΔE according to the given general functional law provides the required sweep for energy subsets $E(n_{ik_n})$. Changing the magnetic field strength B_x, B_y with increment ΔB and/or changing the intensity of the electrostatic field with the step ΔE forming the sequence ($B_{x_1}...B_{x_n}$, $B_{y_1}...B_{y_n}$, $E_{x_1}...E_{x_n}$, $E_{y_1}...E_{y_n}$) thus, there is the set (B_{x_n}, B_{y_n}, $E(n_{ik_n})$, E_{x_n}, E_{y_n}). To is for crossed fields for each individual discrete sequence the aggregate and functionally related values of B_x, B_y or E_{x_n}, E_{y_n} are defined [19; 23].

We present the parameters of the accelerator with a step of adjustment of the accelerating voltage ΔU. Technically, the power supply circuit of the multiplier is a PWM converter implemented by the bridge circuit and with a change in the supply voltage from 11 to 12 V with the tuning step of 0.1 V. This allows the output of the step-up transformer to receive the discrete voltage in the range from

5500 V to 6000 V with the step change of 50 V. Thus, the input voltage on the multiplier changes in the set values.

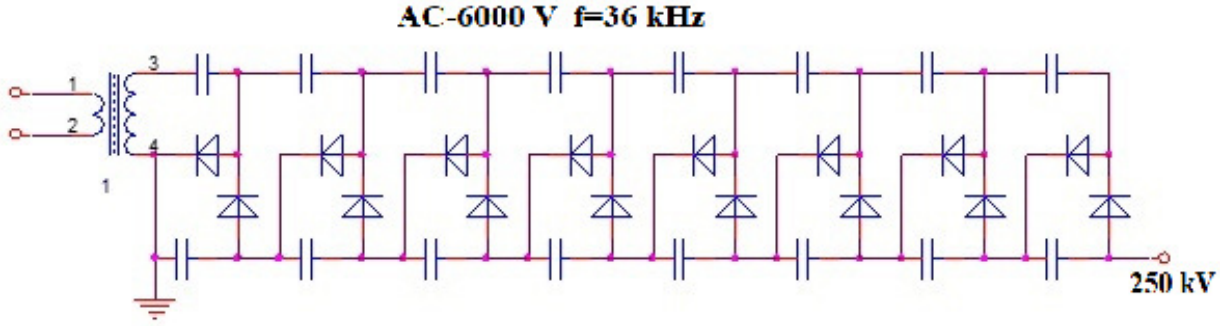

Fig. 2.2. Device scheme for the voltage N-multicascade multiplier

Рис. 2.2. Схема устройства N-многокаскадного умножителя напряжения

To obtain a high voltage, we use an asymmetric voltage multicascade multiplier (Cockcroft–Walton scheme [24]), see Fig. 2.2 with the parameters of the maximum input voltage of 6000 V and the frequency of 36 kHz. Number of multiplier cascades is 22. Capacity of the multiplier capacitors $C = 4.7 \times 10^{-9}$ F. The change in the accelerating voltage in the range from 242 kV to 266 kV for plasma generator with ^{7}Li (and 100 kV for neutron generator). Thus, we have the discrete change in the accelerating voltage at the accelerator, and this allows us to obtain discrete flows of ions or electrons. At the entrance to the magnetic system of the solenoid, we have the distribution along the track radius of discrete ion fluxes with the track radius from R_{i_1} to R_{i_n}. At the same time, in the solenoid system, the movement of the ion flow is carried out along the helical line. The electrons are accelerated in the same way, and then the ion and electron components are combined in the neutralizer chamber. If the energy of electrons and ions is equal, we obtain an equilibrium plasma in which ions and electrons are in a state of thermodynamic quasi-equilibrium, i. e., the temperature of electrons and ions, may be considered, coincides.

Thus, due to the discretization of artificially prepared swirling plasma flows and discrete alternating sequential compaction [25; 26], technically, conditions are created for the implementation of thermonuclear fusion in the considered installation of the plasma generator.

2.1. Klystron-based Quantum Energy Converter

To increase the efficiency of converting the energy of fusion products into electrical energy, it is used in a quantum energy converter (QEC), which is an ion–emission electrovacuum device QEC-2. The resulting helium is injected into the chamber of a quantum energy converter, which is a vacuum flyby klystron in which the energy of helium ions is converted into electrical energy. The operating frequency of the klystron QEC is 12 GHz–25 GHz at an output power of 10 kW from the anodes of the microwave device, the ion stream passes through the input resonator of the device tuned to a frequency of 12–25 GHz and an output resonator for ion energy transfer to microwave power. Quantum energy devices (QED) are powerful microwave vacuum microwave resonator klystrons with an open cathode and an output node powered by an external ion source. Compatible with various electronically controlled plasma generators and used as a powerful converter of high-energy ion energy into microwave oscillations. Powerful vacuum klystrons are designed to amplify high-frequency currents at frequencies from 12.5 GHz to 30 GHz. The microwave resonator klystron is an amplifying electrovacuum microwave device with short–term interaction of an ion flux with the longitudinal component of the sagging electric field of several resonators, using the drift method to modulate the ion flux in density (see Table 2.1). Energy conversion efficiency: 55 % (QEC) vs. 30 % (Zetatron [7]). The output resonator system consists of 4 or 8 resonators connected in parallel to increase power.

Table 2.1

Energy Balance Table

Таблица 2.1

Таблица энергетического баланса

Parameter	**Somov et al. [19]**	**Dolgopolov et al. [18]**	**Patent [20] RU 2757666**	**Ion Klystron**	**SPC NEW ENERGY**
			Input		
Electricity (Power)	1 MWh/cycle	50–500 kW	50–500 kW	1.5 kW	1.5 kW (including LiH heating)
Electricity (Voltage)	Pulse	100 kV	48 V	48 V	48 V
Electricity (Frequency)	Low-frequency	50 Hz	65 kHz	65 kHz	1000 Hz (generator)
Heat (for start)	No	No	No	No	1.2 kW (heating LiH to 850°C, 10 min)
Lithium (Consumption)	10–100 kg/cycle	No	No	No	1g LiH (≈ 3 months operation)
Hydrogen (Consumption)	No	1–5 l/min	No	0.1–1 l/min	1–3 ml/min (helium + α-particles)
			Output		
Electricity (Power)	0.4–0.6 MW	35–350 kW	375–425 kW	50–500 kW (sec pulse)	6.5 kW (sec pulse)
Electricity (Voltage)	AC	DC	DC	DC	DC
Electricity (Frequency)	50 Hz	50 Hz	50 Hz	5–30 GHz (pulse)	153 kHz (KEP)
			Resources		
Component Lifetime	Magnets: 10 years	Electrodes: 2 years	Electrodes: 5 years	Resonators: 5000–25000 hours[1]	LiH: 3 months
			Measurement Methods		
Helium Consumption	No	No	No	Mass flow controllers Mass spectrometry + Langmuir probes	Spectroscopy, electron-optical cameras, Mass spectrometry + Langmuir probes
Plasma Parameters	Hall probes	Spectrometers	Pressure sensors	Laser Doppler anemometry	Divertor plasma diagnostics (He concentration, ion temperature)

[1] The lifetime of the resonators depends on particle energy and bombardment frequency. In the absence of radiation, the resource can reach 25000 hours.

3. Methodology of experimental measurements

3.1. Alpha particle shielding in industrial generators

3.1.1. Physical Basis of Alpha Particle Interaction with Titanium

Let us consider justification of the impossibility of 4.3 MeV helium ions (alpha particles) penetrating 50 μm titanium foil. For the plasma (and neutron aim) generator, a 50 μm titanium foil blocks 4.3 MeV alpha particles (range: 20–25 μm in Ti). SRIM (Stopping and Range of Ions in Matter) simulations confirm full absorption, with perforated steel disks minimizing secondary X-ray interference.

1. Range of alpha particles in materials: alpha particles lose energy mainly due to ionization and elastic collisions with electrons and nuclei. The particle range depends on their energy and the material density.

2. For 4.3 MeV in titanium (density 4.5 g/cm^3), SRIM simulations show a range of approximately 20–25 μm.

3. A titanium foil of 50 μm exceeds the maximum particle range, guaranteeing full stopping.

4. Comparison with experimental data: In aluminum (a less dense material), a 5 μm foil reduces alpha energy from 5.5 MeV to 3.3 MeV (2.2 MeV loss). Extrapolating to titanium shows that 50 μm of titanium is equivalent to $\sim$ 100–120 μm of aluminum, fully preventing particle penetration.

Key Conclusions:

1. Alpha particles with 4.3 MeV energy cannot penetrate 50 μm titanium foil.

2. Any radiation detected beyond the foil is related to perforations in the steel disks or secondary processes (e. g., X-ray emission).

3.2. Photon detection for fusion validation

In this subsection we propose for photon detection from fusion reaction in LiH mixture (90 % ^{7}Li, 10 % ^{6}Li). The $p + {}^7\mathrm{Li} \to 2{}^4\mathrm{He} + \gamma$ reaction produces 8.7 MeV photons (primary signal) and 17 MeV events (rare). While this specific reaction is not typically the focus of large-scale fusion experiments, similar diagnostic approaches for detecting high-energy photons have been employed to confirm thermonuclear conditions in magnetized liner inertial fusion systems [28].

Key spectrometer criteria:

Energy resolution: $\leq$ 1 % FWHM (HPGe) to distinguish 8.7 MeV from $p + {}^{16}O$ background (8–9 MeV).

Efficiency: BGO detectors achieve 25–30 % at 8.7 MeV, suitable for industrial neutron generator monitoring.

Attenuation in titanium: 6 mm Ti transmits 86 % of 8.7 MeV photons (Fig. 3.1).

3.2.1. Photon Energy Spectrum Correction

In the reaction $p + {}^7\mathrm{Li} \to 2{}^4\mathrm{He} + \gamma$, the total energy of 17.3 MeV is shared between the two alpha particles and a photon. Experimentally, the photon carries $\sim$ 8.7 MeV, with the rest transferred to reaction products.

Target energy range: 6–17 MeV, because:

1. Main signal: 8.7 MeV (dominant peak).

2. Additional signals:

- High-energy photons up to 17 MeV (rare full energy release events).
- Background reactions with impurities (O, N in vacuum):
  (a) $p + {}^{14}\mathrm{N} \rightarrow {}^{15}\mathrm{O} + \gamma$ (photons $\sim$ 6–7 MeV).
  (b) $p + {}^{16}\mathrm{O} \rightarrow {}^{17}\mathrm{F} + \gamma$ (photons $\sim$ 8–9 MeV).

3.2.2. Spectrometer Requirements

1. Energy resolution: Must be sufficient to resolve 8.7 MeV peak and background signals (6–9 MeV).
2. Efficiency: High sensitivity in the 6–17 MeV range.
3. Background suppression: Consideration of secondary reactions and cosmic rays (dosimeter reads 20–140 μSv/h).

Comparison of Detectors for the 6–17 MeV Range

1. BGO Detector ($Bi_4Ge_3O_{12}$)
   - Efficiency:
     – High due to material density (7.13 g/cm^3). For 8.7 MeV — $\sim$ 25–30 %, for 17 MeV — $\sim$ 15–20 %.
   - Energy resolution:
     – $\sim$ 8–10 % FWHM at 8.7 MeV (peak width $\sim$ 0.7–0.9 MeV).
     – Peaks at 6–9 MeV may overlap, but statistical analysis allows separation.
   - Advantages:
     – Low cost, radiation resistance.
     – Suitable for detecting rare events up to 17 MeV.
   - Disadvantages:
     – Broad peaks hinder identification of nearby signals (e.g., 8.7 MeV vs 8–9 MeV background).
2. NaI(Tl) Detector
   - Efficiency:
     – For 8.7 MeV — $\sim$ 15–20 %, for 17 MeV — $\sim$ 5–10 %.
   - Energy resolution:
     – $\sim$ 5–6 % FWHM at 8.7 MeV (peak width $\sim$ 0.4–0.5 MeV).
   - Advantages:
     – Better resolution than BGO allows clearer separation of 6–9 MeV peaks.
     – Easy to operate.
   - Disadvantages:
     – Low efficiency for high energies (>10 MeV).
     – Background from natural iodine radioactivity.
3. HPGe Detector (High-Purity Germanium)
   - Efficiency:
     – For 8.7 MeV — $\sim$ 20–25 %, for 17 MeV — $\sim$ 10–15%.
   - Energy resolution:

  - $\sim$ 0.2–0.3 % FWHM at 8.7 MeV (peak width $\sim$ 0.02–0.03 MeV).
- Advantages:
  - Ideal resolution for separating nearby peaks (e.g., 8.7 MeV vs 8–9 MeV).
  - Minimal background.
- Disadvantages:
  - Requires liquid nitrogen cooling.
  - High cost.

Detector Selection Recommendations

Table 3.1

Comparison of BGO, NaI(Tl), and HPGe Detector Characteristics

Таблица 3.1

Сравнение характеристик детекторов BGO, NaI(Tl) и HPGe

Criterion	BGO	NaI(Tl)	HPGe
Efficiency	**Best**	Moderate	Good
Resolution	Low	Moderate	**Excellent**
Background suppression	Requires collimation	Needs shielding	**Automatic**
Cost	Low	Low	High

1. For statistical confirmation of the reaction (rough analysis):
   - BGO is preferable — high efficiency compensates for low resolution.
   - Use lead collimation (thickness $\geq$ 5 cm) to reduce background.
2. For precise spectral analysis:
   - HPGe is preferable — 0.2 % resolution will separate the 8.7 MeV peak from background signals.

Photon Attenuation in Titanium Pipe
Wall thickness: 6 mm. For 8.7 MeV photon:
Attenuation coefficient in titanium: $\mu \approx 0.25$ cm^{-1} (NIST XCOM).
Fraction of transmitted photons: $I/I_0 = e^{-\mu x} = e^{-0.25 \cdot 0.6} \approx 0.86$ (86 %) (Fig. 3.1)

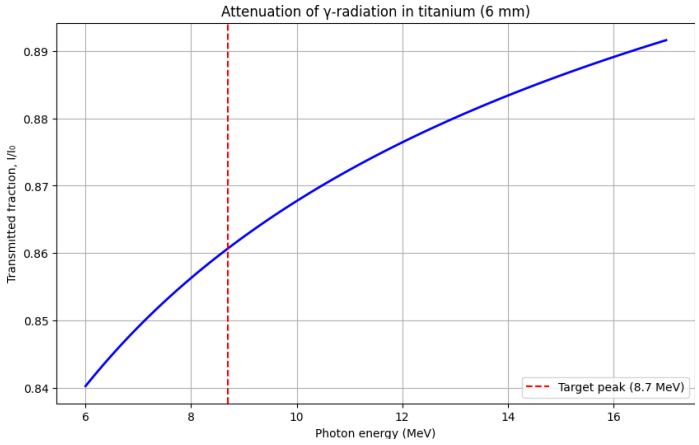

Fig. 3.1. Attenuation of photons in a titanium tube

Рис. 3.1. Ослабление фотонов в титановой трубе

Background Suppression Methods

1. Lead collimation:
   - Reduces the detector's field of view, lowering scattered radiation contributions.
2. Time coincidence:
   - Synchronization of the detector with plasma pulses (reaction is pulsed).
3. Spectral deconvolution:
   - Use algorithms (e.g., Wiener filter) to separate 8.7 MeV peak from background.

Conclusions for methodology

1. The main signal of the $p+^7$Li reaction is 8.7 MeV photons, but the spectrometer should cover 6–17 MeV. Detection of 17.3 MeV photons would confirm the reaction, though statistical confirmation at 8.7 MeV is often sufficient.
2. HPGe is optimal for precise analysis, BGO is suitable for budget experiments. An HPGe detector with collimation is ideal for background suppression and target peak identification.
3. Photon attenuation in titanium is not critical: 86 % of 8.7 MeV photons pass through. 91 % of 17.3 MeV photons are transmitted.
4. To suppress background from O/N reactions, use collimation and data processing.

Final Recommendations

- A 50 μm titanium foil is sufficient to block alpha particles.
- For fusion analysis in LiH (90 % ^{7}Li), use an HPGe spectrometer with correction for titanium attenuation; BGO is suitable for budget setups.
- It is advisable to consider ^{6}Li contribution (4.0 MeV) as background during data processing.

Conclusion

We conclude that in order to solve the problem of controlled synthesis of light nuclei, the technique, and technology for creating and forming electronically controlled ion and plasma fluxes in magnetic fields by grouping flows with sampling and specifying certain sequences laws for ion and plasma fluxes have been developed. The experimental electronically controlled plasma electric generator installation with a vacuum subsystem of blocks and an electronic control system has been assembled. The possibility of using such installations is considered to create serial production of generators of electric and thermal energy for the heat and power supply of enterprises, which is most economically advantageous compared to large reactors. Building autonomous power supply generators based on remote or hard-to-reach residential settlements, autonomous nonvolatile industrial enterprises, and other facilities. Our prototype demonstrates a 40 % cost reduction in isotope production costs compared to TRIGA reactors (12$/gvs.TRIGA's 20 per gram for $^{99m}T_C$) [11] due to the minimized neutron flux dispersion [27].

Recent experiments, such as Gomez et al. [28], demonstrate thermonuclear neutron yields via magnetized liner inertial fusion (MagLIF), achieving up to 2×10^{12} DD neutrons. Our approach, utilizing adaptive plasma discretization, offers higher energy conversion efficiency ($> 50\%$) and modularity, addressing scalability challenges inherent in pulsed-power systems like Z Machine. As shown in the Ragone diagram (Fig. 1.1), our generator outperforms pulsed systems like MagLIF (Z Machine) in energy density, bridging the gap between large-scale fusion and portable solutions.

The Ragoné diagram (Fig. 1.1) illustrates the comparative performance of plasma energy systems and storage technologies, emphasizing power (W) versus energy density (J/kg). The newly developed electronically controlled plasma generator, described in this work, is positioned within the high-efficiency quadrant (>50 % energy conversion), outperforming conventional D-T systems and compact neutron sources. Key innovations, such as lithium hydride evaporation, quadrupole magnetic discretization (Patent RU 2757666 [20]), and adaptive ion flux synchronization, enable the generator to achieve thermal output of 8–25 kW and electrical power of 4–12 kW. These advancements place the system between fusion prototypes (e. g., ITER) and advanced energy storage solutions (e.g., Li-ion batteries) on the diagram (Fig. 1.1), highlighting its modularity and scalability. The inclusion of experimental setups such as the Kurchatov Tokamak and MIFI-MIST series, alongside emerging projects (Helion Fusion's Trenta and TRINITI reactors [31]), underscores the competitive edge of adaptive plasma discretization in bridging the gap between industrial-scale fusion and portable energy systems. When installing neutron protection in the case of neutron generator, it makes sense to use a deuteriumtritium reaction generator on this type, it will be an easy and convenient way to obtain clean energy.

Existing plasma accelerators are divided into thermal and electromagnetic accelerators, the former when acceleration is associated with a drop in total pressure and the latter with Ampere force. In these areas of plasma accelerators, designs are constantly being searched and improved. For example, new developments in plasma accelerators are presented in [31]. But there is another way to obtain accelerated dense plasma, presented in this article, which is to obtain plasma of the required energy from electron and ion plasma components accelerated on separate linear or cyclotron accelerators, followed by their combination to neutralize and produce a plasma flow.

Methodology confirming the plasma generator's operability is considered:

50 μm Ti foils fully block alpha particles, ensuring safety in neutron generator designs.

HPGe detectors resolve 8.7 MeV photons with 0.2 % FWHM, critical for distinguishing fusion signals from $p + O/N$ background.

Future work includes Integration of methodology's protocols into full-scale reactor trials, optimizing photon detection algorithms for real-time monitoring.

Recent advances in non-perturbative guiding center theory (Burby et al., 2025 [32]), which employs machine learning to model high-energy particle dynamics in complex magnetic fields, highlight the importance of data-driven approaches for improving confinement predictions. These developments align with our focus on adaptive ion flux synchronization and could further enhance the accuracy of plasma discretization algorithms in future iterations.

Information about the conflict of interests: authors and reviewers declared no conflicts of interest.

Citation. Chipura A.S., Dolgopolov M.V., Ovchinnikov D.E., Radenko A.V., Radenko V.V. Development of energy converters in discrete ion-plasmodynamic installations with electronic control. *Vestnik Samarskogo universiteta. Estestvennonauchnaya seriya / Vestnik of Samara University. Natural Science Series*, 2025, vol. 31, no. 1, pp. 99–117. DOI: 10.18287/2541-7525-2025-31-1-99-117.

Alexander S. Chipura (al_five@mail.ru) – assistant professor, Department of Higher Mathematics, Institute of Automation and Information Technology, Samara State Technical University, 244, Molodogvardeyskaya Street, 443100, Samara, Russian Federation.

Mikhail V. Dolgopolov (mikhaildolgopolov68@gmail.com) – Candidate of Physical and Mathematical Sciences, associate professor, associate professor of the Department of Higher Mathematics, Institute of Automation and Information Technology, Samara State Technical University, 244, Molodogvardeyskaya Street, 443100, Samara, Russian Federation.

Dmitry E. Ovchinnikov (ovchinnikovde1971@yandex.ru) – Doctor of Economics, professor, Vice-Rector, Vice-Rector for Academic Affairs, Samara State Technical University, 244, Molodogvardeyskaya Street, 443100, Samara, Russian Federation.

Alexander V. Radenko (avradenko@ya.ru) – chief technologist, Scientific and Production Company "New Energy" LLC, 25/2, Zavodskoye shosse, Samara, 443022, Russian Federation.
Vitaly V. Radenko (tp-aist@mail.ru) – chief designer, Scientific and Production Company "New Energy" LLC, 25/2, Zavodskoye shosse, Samara, 443022, Russian Federation.

References

[1] Uesaka M., Kobayashi H. Compact Neutron Sources for Energy and Security. *Reviews of Accelerator Science and Technology*, 2015, vol. 08, pp. 181–207. DOI: https://doi.org/10.1142/S1793626815300108.

[2] Leung K.N., Leung J.K., Melville G. Feasibility study on medical isotope production using a compact neutron generator. *Applied Radiation and Isotopes*, 2018, vol. 137, pp. 23–27. DOI: https://doi.org/10.1016/j.apradiso.2018.02.026.

[3] Battermann J.J., Mijnheer B.J. The amsterdam fast neutron therapy project: A final report. *International Journal of Radiation Oncology Biology Physics*, 1986, vol. 12, issue 12, pp. 2093–2099. DOI: https://doi.org/10.1016/0360-3016(86)90007-6.

[4] Kreiner A.J. et al. Present status of Accelerator-Based BNCT. *Reports of Practical Oncology & Radiotherapy*, 2016, vol. 21, issue 2, pp. 95–101. DOI: https://doi.org/10.1016/j.rpor.2014.11.004.

[5] Metwally W.A. et al. Utilizing neutron generators in boron neutron capture therapy. *Applied Radiation and Isotopes*, 2021, vol. 174, p. 109742. DOI: https://doi.org/10.1016/j.apradiso.2021.109742.

[6] Leung K.N. New Compact Neutron Generator System for Multiple Applications. *Nuclear Technology*, 2020, vol. 206, issue 10, pp. 1607–1614. DOI: https://doi.org/10.1080/00295450.2020.1719800.

[7] Shope L.A. et al. Operation and Life of the Zetatron: A Small Neutron Generator for Borehole Logging. *IEEE Transactions on Nuclear Science*, 1981, vol. 28, issue 2, pp. 1696–1699. DOI: http://doi.org/10.1109/TNS.1981.4331501.

[8] Altukhov A.A. et al. Monitoring the yield of a borehole neutron generator. *Russian Engineering Research*, 2016, vol. 36, pp. 607-–610. DOI: https://doi.org/10.3103/S1068798X16070030.

[9] Shimura F. Single-Crystal Silicon: Growth and Properties. In: Kasap, S., Capper, P. (eds) Springer Handbook of Electronic and Photonic Materials. Springer Handbooks. Springer, Boston, MA., 2017, pp. 255–269. DOI: https://doi.org/10.1007/978-0-387-29185-7_13.

[10] Chichester D., Simpson J., Lemchak M. Advanced compact accelerator neutron generator technology for active neutron interrogation field work. *Journal of Radioanalytical and Nuclear Chemistry*, 2007, vol. 271, issue 3, pp. 629–637. DOI: https://doi.org/10.1007/s10967-007-0318-7.

[11] Mausolf E.J. et al. Fusion-Based Neutron Generator Production of Tc-99m and Tc-101: A Prospective Avenue to Technetium Theranostics. *Pharmaceuticals*, 2021, vol. 14, issue 9, p. 875. DOI: https://doi.org/10.3390/ph14090875.

[12] Pudjorahardjo D.S., Wahyono P.I., Syarip. Compact neutron generator as external neutron source of subcritical assembly for Mo-99 production (SAMOP). *AIP Conference Proceedings*, 2020, vol. 2296, issue 1, p. 020115. DOI: https://doi.org/10.1063/5.0030345.

[13] Brown I.J. The Physics and Technology of Ion Sources, 2nd Revised and Extended Edition. Wiley-VCH, 2004, 396 p.

[14] Mesyats Gennady A. Pulsed power. Springer, 2005. 568 p. DOI: https://doi.org/10.1007/b116932.

[15] Forrester A.T. Large Ion Beams: Fundamentals of Generation and Propagation. *Physics Today*, 1989, vol. 42, issue 6, pp. 77–78. DOI: https://doi.org/10.1063/1.2811058.

[16] Akimchenko A. et al. Betavoltaic device in por-SiC/Si C-Nuclear Energy Converter. *EPJ Web of Conferences*, 2017, vol. 158, Article number 06004. DOI: https://doi.org/10.1051/epjconf/201715806004.

[17] Datta R. et al. Radiatively Cooled Magnetic Reconnection Experiments Driven by Pulsed Power. *Physics of Plasmas*, 2024, vol. 31, issue 5, p. 052110. DOI: https://doi.org/10.1063/5.0201683.

[18] Dolgopolov M.V., Radenko V.V., Zanin G.G., Ovchinnikov D.E., Radenko A.V., Svirkov V.B., Chipura A.S., Gurskaya A.V. Electronically Controlled Plasma Power Devices for Sustainable and Environmentally Friendly Electric Energy Technologies. *Advances in Engineering Research. Volume 210. Proceedings of the Conference on Broad Exposure to Science and Technology 2021 (BEST 2021)*. Atlantis Press, 2021, pp. 197–205. DOI: http://doi.org/10.2991/aer.k.220131.033.

[19] Somov A.I., Radenko V.V., Svirkov V.B., Dolgopolov M.V., Vasiliev I.V., Bagrov A.R. On the Possibility of Initialization of Synthesis in Small-sized Installations with Quadrupole Magnetic Systems with Spherical Cumulation of Shock Magnetic Waves in the Blanket Configuration of Plasma Discrets. *Computational Nanotechnology*, 2023, vol. 10, issue 2, pp. 70–88. DOI: https://doi.org/10.33693/2313-223X-2023-10-2-70-88. (In Russ.)

[20] Dolgopolov M.V., Zanin G.G., Ovchinnikov D.E., Radenko V.V., Svirkov V.B. Patent RU 2 757 666 C1, 20.10.2021. Electronically controlled plasma electric generator. No. 2021105186 dated 01.03.2021. Available at: https://yandex.ru/patents/doc/RU2757666C1_20211020?ysclid=m98552hxjf308596075. (In Russ.)

[21] Burtebaev N. et al. Systematic Study of the p, d and 3He Elastic Scattering on 6Li. *International Journal of Physical and Mathematical Sciences*, 2011, vol. 5, no. 2, pp. 73–75. DOI: https://doi.org/10.5281/zenodo.1076606.

[22] Elisov M.V. Lithium ions with energy 250-360 keV in the system of solenoidal and quadrupole magnetic fields. *9th International School and Conference on Optoelectronics, Photonics, Engineering and Nanostructures*. Saint Petersburg, 2022, pp. 590–591. Available at: https://www.elibrary.ru/item.asp?id=55666293. EDN: https://www.elibrary.ru/sxyzii.

[23] Dolgopolov M., Gurskaya A., Privalov A., Radenko V., Radenko A., Svirkov V. Electronically driven neutrons synthesis-generator with the magneto-optical flow seal. *EPJ Web of Conferences. The XXIV International Workshop "High Energy Physics and Quantum Field Theory" (QFTHEP 2019)*, 2019, vol. 222, Article number 02014. DOI: https://doi.org/10.1051/epjconf/201922202014.

[24] Cockcroft J.D., Walton E.T.S. Experiments with High Velocity Positive Ions. (I) Further Developments in the Method of Obtaining High Velocity Positive Ions. *Proceedings of the Royal Society A*, 1932, vol. 136, pp. 619–630. DOI: http://dx.doi.org/10.1098/rspa.1932.0107.

[25] Dolgopolov M.V., Zanin G.G., Radenko A.V., Radenko V.V., Svirkov V.B. Mathematical modeling of ion and plasma multiphase flow in the plasma electric synthesis generator. In: *Mathematical modeling and boundary value problems: Proceedings of the XI All-Russian scientific conference with international participation: in 2 vol. Vol. 1.* Samara: Samarskii gosudarstvennyi tekhnicheskii universitet, 2019, pp. 258–263. Available at: https://www.elibrary.ru/item.asp?id=38559765. EDN: https://www.elibrary.ru/unwnjf. (In Russ.)

[26] Chepurnov V.I., Dolgopolov M.V., Gurskaya A.V., Akimchenko A.A., Kuznetsov O.V., Radenko A.V., Radenko V.V., Mashnin A.S. C-betavoltaic energyconverter in por-SiC/Si. *Materials Science. Non-Equilibrium Phase Transformations*, 2017, year III, issue 3, pp. 119–120. Available at: https://www.researchgate.net/publication/386111461_C-betavoltaic_energyconverter_in_por-SiCSi.

[27] Radenko V.V., Dolgopolov M.V., Chipura A.S., Radenko A.V., Svirkov V.B., Somov A.I. Plasma neutron generator on a plasma target for activation semiconductor materials. *Physics of Particles and Nuclei*, 2025, vol. 56, no. 3.

[28] Gomez M.R. et al. Demonstration of thermonuclear conditions in magnetized liner inertial fusion experiments. *Physics of Plasmas*, 2015, vol. 22, no. 5, pp. 056306. DOI: https://doi.org/10.1063/1.4919394.

[29] Hsu S.C. et al. Progress toward fusion energy breakeven and gain as measured against the Lawson criterion. *Phys. Plasmas*, 2022, vol. 29 (6), pp. 062103. DOI: https://doi.org/10.1063/5.0083990.

[30] Lerner E.J. et al. Focus fusion: overview of progress towards p-B^{11} fusion with the dense plasma focus. *J. Fusion Energ*, 2023, vol. 42, pp. 7. DOI: https://doi.org/10.1007/s10894-023-00345-z.

[31] Zhitlukhin A.M. The current state of research on pulsed thermonuclear devices based on dense magnetized plasma flows. *Open Scientific seminar Controlled Thermonuclear Fusion and Plasma Technologies, conducted by Rosatom State Corporation on June 30*, 2023. Available at: https://fusion.rosatom.ru/upload/iblock/421/421898e77a472e4670493568677e3831.pdf abstracts and presentations. SSC RF TRINITI.

[32] Burby J.W., Maldonado I.A., Ruth M., et al. Nonperturbative Guiding Center Model for Magnetized Plasmas. *Phys. Rev. Lett*, 2025, vol. 134, pp. 175101. DOI: https://doi.org/10.1103/PhysRevLett.134.175101.

DOI: 10.18287/2541-7525-2025-31-1-99-117 УДК 533.9.07; 533.95; 533.933

Развитие преобразователей энергии в дискретных ионно-плазмодинамических установках с электронным управлением

Чипура*[1] *А.С.*, *Долгополов*[1] *М.В.*, *Овчинников*[1] *Д.Е.*, *Раденко*[2] *А.В.*, *Раденко*[2] *В.В.

[1] *Самарский государственный технический университет, г. Самара, Российская Федерация; al_five@mail.ru; ORCID: 0009-0004-0425-0653 (А.С.); mikhaildolgopolov68@gmail.com; ORCID: 0000-0002-8725-7831 (М.В.); ovchinnikovde1971@yandex.ru; ORCID: 0000-0001-7934-5105 (Д.Е.);*

[2] *Научно-производственная компания "Новая энергия" ООО, г. Самара, Российская Федерация; avradenko@ya.ru; ORCID: 0009-0001-0404-2385 (А.В.); tp-aist@mail.ru; ORCID: 0009-0008-3353-2667 (В.В.);*

Поступила: 16.12.2024
Рассмотрена: 18.04.2025
Принята: 07.04.2025

Научная статья

Аннотация. Разработаны методы создания электронно-управляемых потоков ионов и плазмы в магнитных полях для нейтронного генератора, плазменного электрогенератора и генератора на основе клистрона. Методика и технология создания и формирования электронно-управляемых потоков ионов и плазмы в магнитных полях были разработаны для реализации управляемого термоядерного синтеза посредством адаптивной дискретной модуляции потоков. Работа блоков установок основана на принципах уплотнения плазмы с магнито-оптической синхронизацией в реальном времени, критически важной для минимизации потерь на циклотронное излучение. В работе представлена комплексная методология экспериментальной валидации, включающая детектирование высокоэнергетических фотонов (6–17 МэВ) и экранирование альфа-частиц титановой фольгой толщиной 50 мкм, необходимые для испытаний промышленных плазменных генераторов. Рассмотрены теоретические и прикладные аспекты моделирования магнитодинамических потоков плазмы, а также новая конструкция плазменного нейтронного генератора с динамической плазменной мишенью. Предложенный электронно-управляемый генератор-преобразователь энергии плазмы демонстрирует тепловую мощность 8–25 кВт и электрическую мощность 4–12 кВт, превышая эффективность преобразования энергии (>50 %) традиционных D-T систем. Предлагается нейтронный генератор с плазменной мишенью, обеспечивающий импульсный поток до 10^{10} $с^{-1}$, что демонстрирует преимущества по сравнению с традиционными D-T системами. Использование компактных нейтронных и электрогенераторов позволяет преодолеть ограничения традиционных ядерных реакторов деления, обеспечивая модульность и быструю масштабируемость. Недавние разработки включают импульсные D-T генераторы и гибридные лазерно-плазменные системы, однако эффективность преобразования энергии в них остаётся низкой (<30%). Плазменный электрический генератор реализован на основе испарения гидрида лития и квадрупольной магнитной дискретизации (Патент RU 2757666). Технология решает проблему масштабируемости традиционных реакторов деления, предлагая модульность и быстрое развертывание, с перспективой применения в производстве изотопов и в компактных нейтронных источниках.

Ключевые слова: квадрупольные магнитные системы; электростатическое ускорение; магнитная линза; плазменная мишень; термоядерный синтез; плазменные токи; синхронизация; генератор синтеза; нейтронный генератор; клистрон; гамма-спектроскопия.

Информация о конфликте интересов: авторы и рецензенты заявляют об отсутствии конфликта интересов.

Цитирование. Chipura A.S., Dolgopolov M.V., Ovchinnikov D.E., Radenko A.V., Radenko V.V. Development of energy converters in discrete ion-plasmodynamic installations with electronic control // Вестник Самарского университета. Естественнонаучная серия / Vestnik of Samara University. Natural Science Series 2025. Т. 31, № 1. С. 99–117. DOI: 10.18287/2541-7525-2025-31-1-99-117.

Александр Сергеевич Чипура (al_five@mail.ru) – ассистент кафедры высшей математики, институт автоматики и информационных технологий, Самарский государственный технический университет, 443100, Российская Федерация, г. Самара, ул. Молодогвардейская, 244.
Михаил Вячеславович Долгополов (mikhaildolgopolov68@gmail.com) – кандидат физико-математических наук, доцент, доцент кафедры высшей математики, институт автоматики и информационных технологий, Самарский государственный технический университет, 443100, Российская Федерация, г. Самара, ул. Молодогвардейская, 244.
Дмитрий Евгеньевич Овчинников (ovchinnikovde1971@yandex.ru) – доктор экономических наук, профессор, первый проректор — проректор по учебной работе, Самарский государственный технический университет, 443100, Российская Федерация, г. Самара, ул. Молодогвардейская, 244.
Александр Владимирович Раденко (avradenko@ya.ru) – главный технолог, НПК "Новая энергия ООО", 443022, Самара, Заводское шоссе, 25/2.
Виталий Владимирович Раденко (tp-aist@mail.ru) – главный конструктор, НПК "Новая энергия ООО", 443022, Самара, Заводское шоссе, 25/2.

Литература

[1] Uesaka M., Kobayashi H. Compact Neutron Sources for Energy and Security // Reviews of Accelerator Science and Technology. 2015. Vol. 08. P. 181–207. DOI: https://doi.org/10.1142/S1793626815300108.

[2] Leung K.N., Leung J.K., Melville G. Feasibility study on medical isotope production using a compact neutron generator // Applied Radiation and Isotopes, 2018. Vol. 137. P. 23–27. DOI: https://doi.org/10.1016/j.apradiso.2018.02.026.

[3] Battermann J.J., Mijnheer B.J. The amsterdam fast neutron therapy project: A final report // International Journal of Radiation Oncology Biology Physics. 1986. Vol. 12, issue 12. P. 2093–2099. DOI: https://doi.org/10.1016/0360-3016(86)90007-6.

[4] Kreiner A.J. et al. Present status of Accelerator-Based BNCT // Reports of Practical Oncology & Radiotherapy. 2016. Vol. 21, issue 2. P. 95–101. DOI: https://doi.org/10.1016/j.rpor.2014.11.004.

[5] Metwally W.A. et al. Utilizing neutron generators in boron neutron capture therapy // Applied Radiation and Isotopes. 2021. Vol. 174. P. 109742. DOI: https://doi.org/10.1016/j.apradiso.2021.109742.

[6] Leung K.N. New Compact Neutron Generator System for Multiple Applications // Nuclear Technology. 2020. Vol. 206, issue 10. P. 1607–1614. DOI: https://doi.org/10.1080/00295450.2020.1719800.

[7] Shope L.A. et al. Operation and Life of the Zetatron: A Small Neutron Generator for Borehole Logging // IEEE Transactions on Nuclear Science. 1981. Vol. 28, issue 2. P. 1696–1699. DOI: http://doi.org/10.1109/TNS.1981.4331501.

[8] Altukhov A.A. et al. Monitoring the yield of a borehole neutron generator // Russian Engineering Research. 2016. Vol. 36. P. 607-–610. DOI: https://doi.org/10.3103/S1068798X16070030.

[9] Shimura F. Single-Crystal Silicon: Growth and Properties. In: Kasap, S., Capper, P. (eds.) Springer Handbook of Electronic and Photonic Materials. Springer Handbooks. Springer, Boston, MA. 2017. P. 255–269. DOI: https://doi.org/10.1007/978-0-387-29185-7_13.

[10] Chichester D., Simpson J., Lemchak M. Advanced compact accelerator neutron generator technology for active neutron interrogation field work // Journal of Radioanalytical and Nuclear Chemistry. 2007. Vol. 271, issue 3. P. 629-–637. DOI: https://doi.org/10.1007/s10967-007-0318-7.

[11] Mausolf E.J. et al. Fusion-Based Neutron Generator Production of Tc-99m and Tc-101: A Prospective Avenue to Technetium Theranostics // Pharmaceuticals. 2021. Vol. 14, issue 9. P. 875. DOI: https://doi.org/10.3390/ph14090875.

[12] Pudjorahardjo D.S., Wahyono P.I., Syarip. Compact neutron generator as external neutron source of subcritical assembly for Mo-99 production (SAMOP) // AIP Conference Proceedings. 2020. Vol. 2296, issue 1. P. 020115. DOI: https://doi.org/10.1063/5.0030345.

[13] Brown I.J. The Physics and Technology of Ion Sources, 2nd Revised and Extended Edition. Wiley-VCH, 2004. 396 p.

[14] Mesyats Gennady A. Pulsed power. Springer, 2005. 568 p. DOI: https://doi.org/10.1007/b116932.

[15] Forrester A.T. Large Ion Beams: Fundamentals of Generation and Propagation // Physics Today. 1989. Vol. 42, issue 6. P. 77–78. DOI: https://doi.org/10.1063/1.2811058.

[16] Akimchenko A. et al. Betavoltaic device in por-SiC/Si C-Nuclear Energy Converter // EPJ Web of Conferences. 2017. Vol. 158. Article number 06004. DOI: https://doi.org/10.1051/epjconf/201715806004.

[17] Datta R. et al. Radiatively Cooled Magnetic Reconnection Experiments Driven by Pulsed Power // Physics of Plasmas. 2024. Vol. 31, issue 5. P. 052110. DOI: https://doi.org/10.1063/5.0201683.

[18] Dolgopolov M.V., Radenko V.V., Zanin G.G., Ovchinnikov D.E., Radenko A.V., Svirkov V.B., Chipura A.S., Gurskaya A.V. Electronically Controlled Plasma Power Devices for Sustainable and Environmentally Friendly Electric Energy Technologies // Advances in Engineering Research. Vol. 210. Proceedings of the Conference on Broad Exposure to Science and Technology 2021 (BEST 2021). Atlantis Press, 2021. P. 197—205. DOI: http://doi.org/10.2991/aer.k.220131.033.

[19] Сомов А.И., Свирков В.Б., Раденко В.В., Долгополов М.В., Васильев И.В., Багров А.Р. О возможности инициализации синтеза в малогабаритных установках с квадрупольными магнитными системами со сферической кумуляцией ударных магнитных волн в бланкетной конфигурации дискретов плазмы // Computational nanotechnology. 2023. Т. 10, вып. 2. С. 70—88. DOI: https://doi.org/10.33693/2313-223X-2023-10-2-70-88.

[20] Электронно-управляемый плазменный электрический генератор / Долгополов М.В., Занин Г.Г., Овчинников Д.Е., Раденко А.В., Раденко В.В., Свирков В.Б. Патент на изобретение RU 2 757 666 C1, 20.10.2021. Заявка № 2021105186 от 01.03.2021. URL: https://yandex.ru/patents/doc/RU2757666C1_20211020?ysclid=m98552hxjf308596075.

[21] Burtebaev N. et al. Systematic Study of the p, d and 3He Elastic Scattering on 6Li // International Journal of Physical and Mathematical Sciences. 2011. Vol. 5, no. 2, P. 73–75. DOI: https://doi.org/10.5281/zenodo.1076606.

[22] Elisov M.V. Lithium ions with energy 250-360 keV in the system of solenoidal and quadrupole magnetic fields // 9th International School and Conference on Optoelectronics, Photonics, Engineering and Nanostructures. Saint Petersburg, 2022. P. 590–591. URL: https://www.elibrary.ru/item.asp?id=55666293. EDN: https://www.elibrary.ru/sxyzii.

[23] Dolgopolov M., Gurskaya A., Privalov A., Radenko V., Radenko A., Svirkov V. Electronically driven neutrons synthesis-generator with the magneto-optical flow seal // EPJ Web of Conferences. The XXIV International Workshop "High Energy Physics and Quantum Field Theory" (QFTHEP 2019). 2019. Vol. 222, Article number 02014. DOI: https://doi.org/10.1051/epjconf/201922202014.

[24] Cockcroft J.D., Walton E.T.S. Experiments with High Velocity Positive Ions. (I) Further Developments in the Method of Obtaining High Velocity Positive Ions // Proceedings of the Royal Society A, 1932. Vol. 136. P. 619–630. DOI: http://dx.doi.org/10.1098/rspa.1932.0107.

[25] Долгополов М.В., Занин Г.Г., Раденко А.В. и др. Математическое моделирование ионного многофазного потока в плазменном электрическом синтез-генераторе // Математическое моделирование и краевые задачи: материалы XI Всероссийской научной конференции с международным участием: в 2 т. Т. 1. Самара: Самарский государственный технический университет, 2019. С. 258–263. URL: https://www.elibrary.ru/item.asp?id=38559765. EDN: https://www.elibrary.ru/unwnjf.

[26] Chepurnov V.I., Dolgopolov M.V., Gurskaya A.V., Akimchenko A.A., Kuznetsov O.V., Radenko A.V., Radenko V.V., Mashnin A.S. C-betavoltaic energyconverter in por-SiC/Si // Materials Science. Non-Equilibrium Phase Transformations. 2017. Year III. Issue 3. P. 119–120. URL: https://www.researchgate.net/publication/386111461_C-betavoltaic_energyconverter_in_por-SiCSi.

[27] Раденко В.В., Долгополов М.В., Чипура А.С., Раденко А.В., Свирков В.Б., Сомов А.И. Плазменный нейтронный генератор на плазменной мишени для активации полупроводниковых материалов // Физика элементарных частиц и атомного ядра. 2025. Т. 56, вып. 3.

[28] Gomez M.R. et al. Demonstration of thermonuclear conditions in magnetized liner inertial fusion experiments // Physics of Plasmas. 2015. Vol. 22, № 5. P. 056306. DOI: https://doi.org/10.1063/1.4919394.

[29] Hsu S.C. et al. Progress toward fusion energy breakeven and gain as measured against the Lawson criterion // Phys. Plasmas 2022. Vol. 29 (6). P. 062103. DOI: https://doi.org/10.1063/5.0083990.

[30] Lerner E.J. et al. Focus fusion: overview of progress towards p-B^{11} fusion with the dense plasma focus // J. Fusion Energ. 2023. Vol. 42. P. 7. DOI: https://doi.org/10.1007/s10894-023-00345-z.

[31] Житлухин А.М. Современное состояние исследований импульсных термоядерных устройств на базе потоков плотной замагниченной плазмы // Открытый научный семинар "Управляемый термоядерный синтез и плазменные технологии", проведённый Госкорпорацией "Росатом" 30 июня 2023 года: тезисы, доклады. ГНЦ РФ ТРИНИТИ. URL: https://fusion.rosatom.ru/upload/iblock/421/421898e77a472e4670493568677e3831.pdf abstracts and presentations. SSC RF TRINITI.

[32] Burby J.W., Maldonado I.A., Ruth M., et al. Nonperturbative Guiding Center Model for Magnetized Plasmas // Phys. Rev. Lett. 2025. Vol. 134. P. 175101. DOI: https://doi.org/10.1103/PhysRevLett.134.175101.